

Supplementary

The GATA-type transcription factor Csm1 regulates conidiation and secondary metabolism in *Fusarium fujikuroi*

Eva-Maria Niehaus^{1¶}, Julia Schumacher¹, Immo Burkhardt², Patrick Rabe², Eduard Spitzer¹, Martin Münsterkötter³, Ulrich Güldener⁴, Christian M. K. Sieber⁵, Jeroen S. Dickschat², Bettina Tudzynski^{1*}

¹Institut für Biologie und Biotechnologie der Pflanzen, Westfälische Wilhelms-Universität Münster, Münster, Germany

²Kekulé-Institut für Organische Chemie und Biochemie, Rheinische Friedrich-Wilhelms-Universität Bonn, Bonn, Germany

³Institute of Bioinformatics and Systems Biology, Helmholtz Zentrum München, German Research Center for Environmental Health (GmbH), Neuherberg, Germany

⁴Department of Genome-oriented Bioinformatics, Wissenschaftszentrum Weihenstephan, Technische Universität München, Freising, Germany

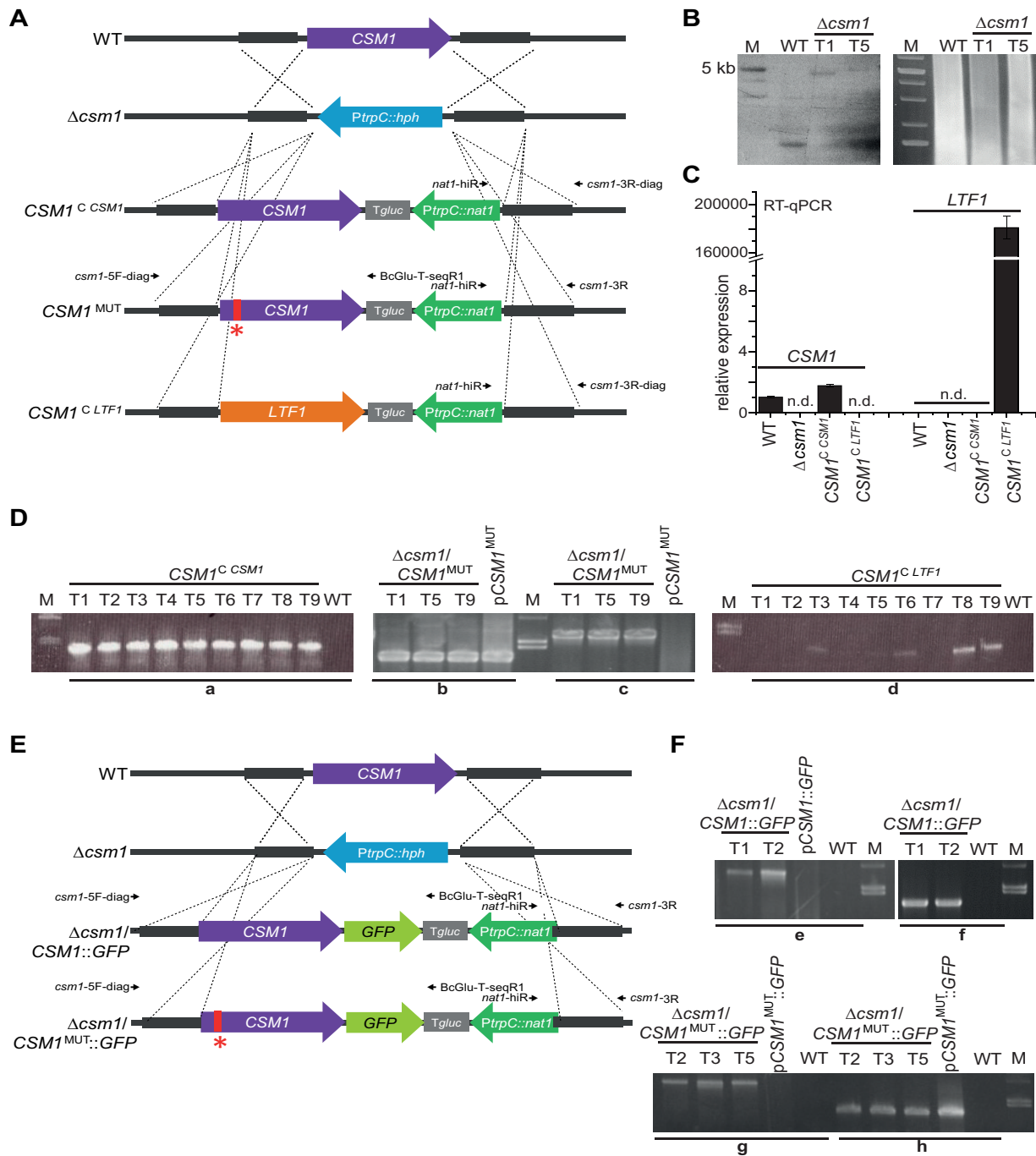
⁵Department of Energy Joint Genome Institute, Walnut Creek, California, United States of America

[¶]Present address: Institute of Food Chemistry, Westfälische Wilhelms-Universität Münster, Münster, Germany

CORRESPONDENCE:

Prof. Dr. B. Tudzynski
tudzynsb@uni-muenster.de

1



2

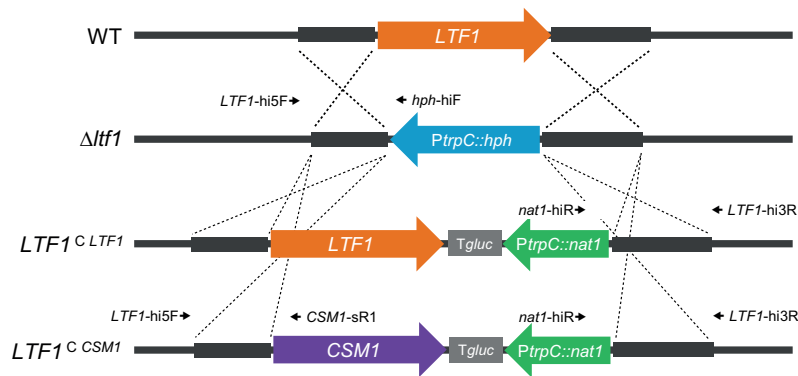
Figure S1: Strategies for functional analysis of *CSM1* and the conserved RQSLPSI motif. (A) All fragments were introduced into the *CSM1* locus of the $\Delta csm1$ mutant by homologous recombination. The red asterisk shows the change of three nucleotides of the putative motif 5'-CGCCAGTCGCTGCCCTCAATC-3' (RQSLPSI) into the following sequence: 5'-GGCCAGGCGCTGCCCGCAATC-3' (GQALPAI). **(B)** Southern blot of the WT and $\Delta csm1$ strains T1 and T5. Genomic DNA was digested with *Hind*III resulting in hybridizing fragments of 1.4 kb (WT) and 4.6 kb ($\Delta csm1$), M = Gene Ruler 1 kb Plus Ladder. **(C)** Gene expression of *CSM1* and *LTF1* in WT, $\Delta csm1$, and complemented strains. RT-qPCR was performed using cDNA derived from cultures grown for three days in ICI medium supplemented with 6 mM glutamine. The level in the WT was defined as 1. Mean value and standard deviation are derived from two replicates. **(D)** Diagnostic PCR of *CSM1^C* mutants, a: *nat1*-hiR + *csm1*-3R-diag (1.6 kb), T1 and T2 were chosen for further experiments; diagnostic PCR of $\Delta csm1$ /*CSM1^{MUT}*, b: *nat1*-hiR + *csm1*-3R (1.5 kb) c: *csm1*-5F-diag + *BcGlu*-T-seqR1 (2.6 kb); diagnostic PCR of *CSM1^C LTF1*, d: *nat1*-hiR + *csm1*-3R-diag (1.6 kb), T6 and T8 were chosen

1 for further experiments; M= λ /HindIII (4.4, 2.3 and 2.0 kb). **(E)** Strategy for insertion of *GFP* constructs.
2 **(F)** Diagnostic PCR of $\Delta csmI/CSMI::GFP$, e: csm1-5F-diag + BcGlu-T-seqR1 (3.3 kb), f: nat1-hiR +
3 csm1-3R (1.5 kb); diagnostic PCR of $\Delta csmI/CSMI^{MUT}::GFP$, g: csm1-5F-diag + BcGlu-T-seqR1
4 (3.3 kb) h: nat1-hiR + csm1-3R (1.5 kb); M = λ /HindIII (4.4, 2.3 and 2.0 kb).

5

6

A



B

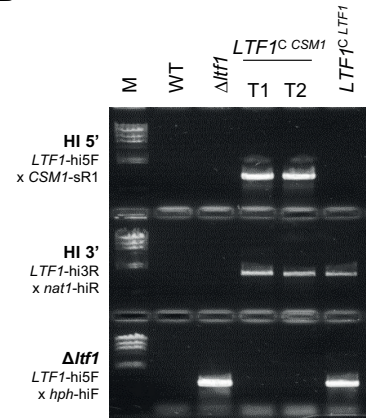


Figure S2: Integration of *CSM1* at the *B. cinerea* *LTF1* locus. (A) Strategy of mutant construction. *CSM1* was introduced at *LTF1* by replacement of the hygromycin resistance cassette according to the strategy used for the complementation of the $\Delta ltf1$ mutant ($LTF1^C LTF1$) in a previous study. **(B)** Diagnostic PCR confirmed the targeted integration of *CSM1*. Primer combinations as indicated were used to detect the homologous integration at 5' and 3' of *LTF1*. Furthermore, the homokaryotic status of the $LTF1^C CSM1$ mutants (T1, T2) was demonstrated (absence of $\Delta ltf1$ allele).

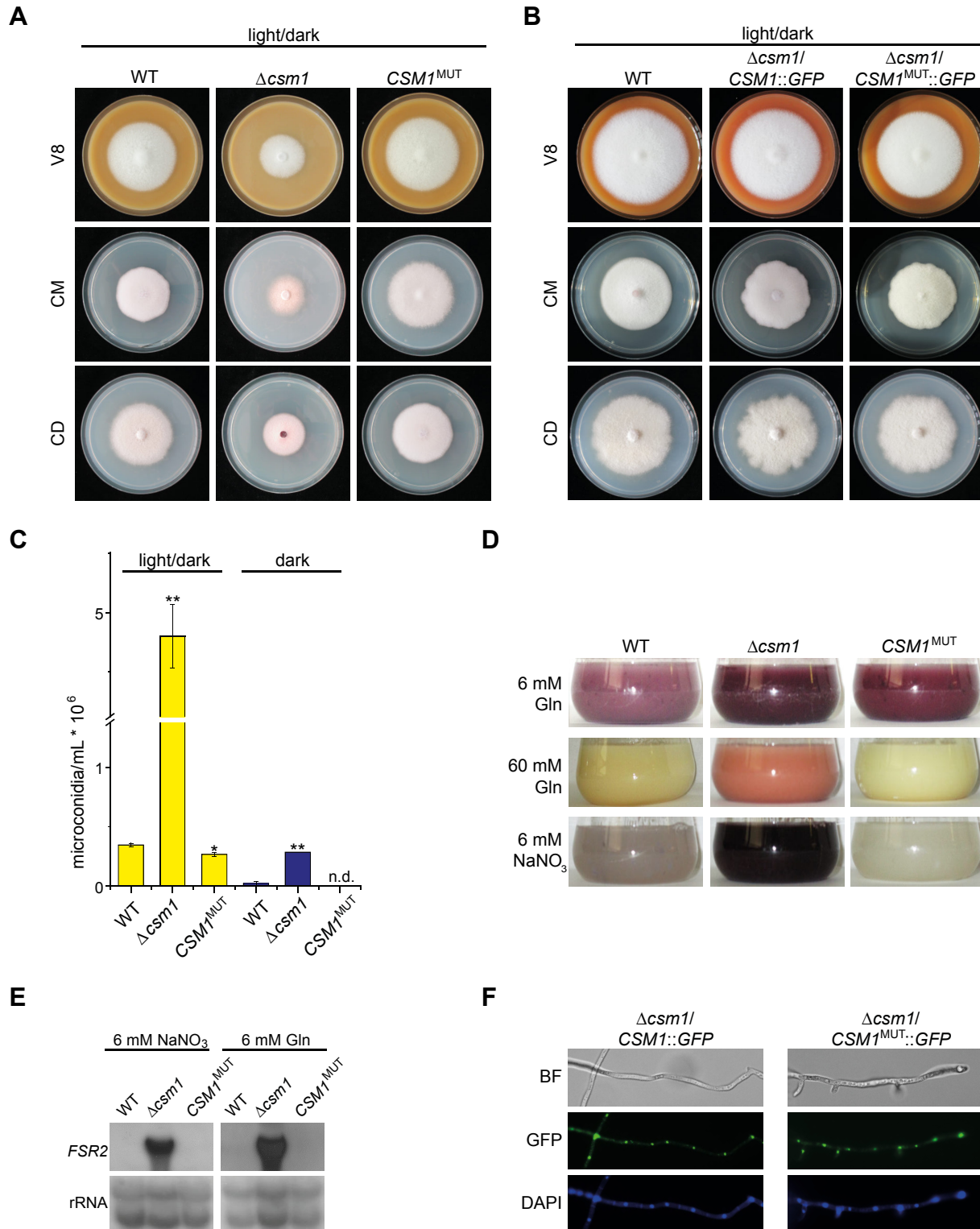


Figure S3: Complementation of the $\Delta csm1$ mutant with the mutated $CSM1$ copy. (A) Colony morphology after 5 d. (B) Colony morphology after 6 d. (C) Number of microconidia produced in light/dark (12h/12h) and in the dark. Mean values and standard deviations shown derived from three biological replicates. Statistical tests (t-test) revealed significant differences (* $p < 0.05$, ** $p < 0.001$). (D) Pigmentation of the cultures. (E) Northern blot analysis of WT, $\Delta csm1$ and $CSM1^{MUT}$ grown in 6 mM $NaNO_3$ or 6 mM glutamine (Gln) for 2 d. The *O*-methyltransferase *FSR2* was used as probe. (F) The subcellular localization of the Csm1 and Csm1^{MUT}-GFP fusion constructs by fluorescent microscopy (GFP). Nuclei were visualized by using Hoechst solution for staining (DAPI); BF = bright field.

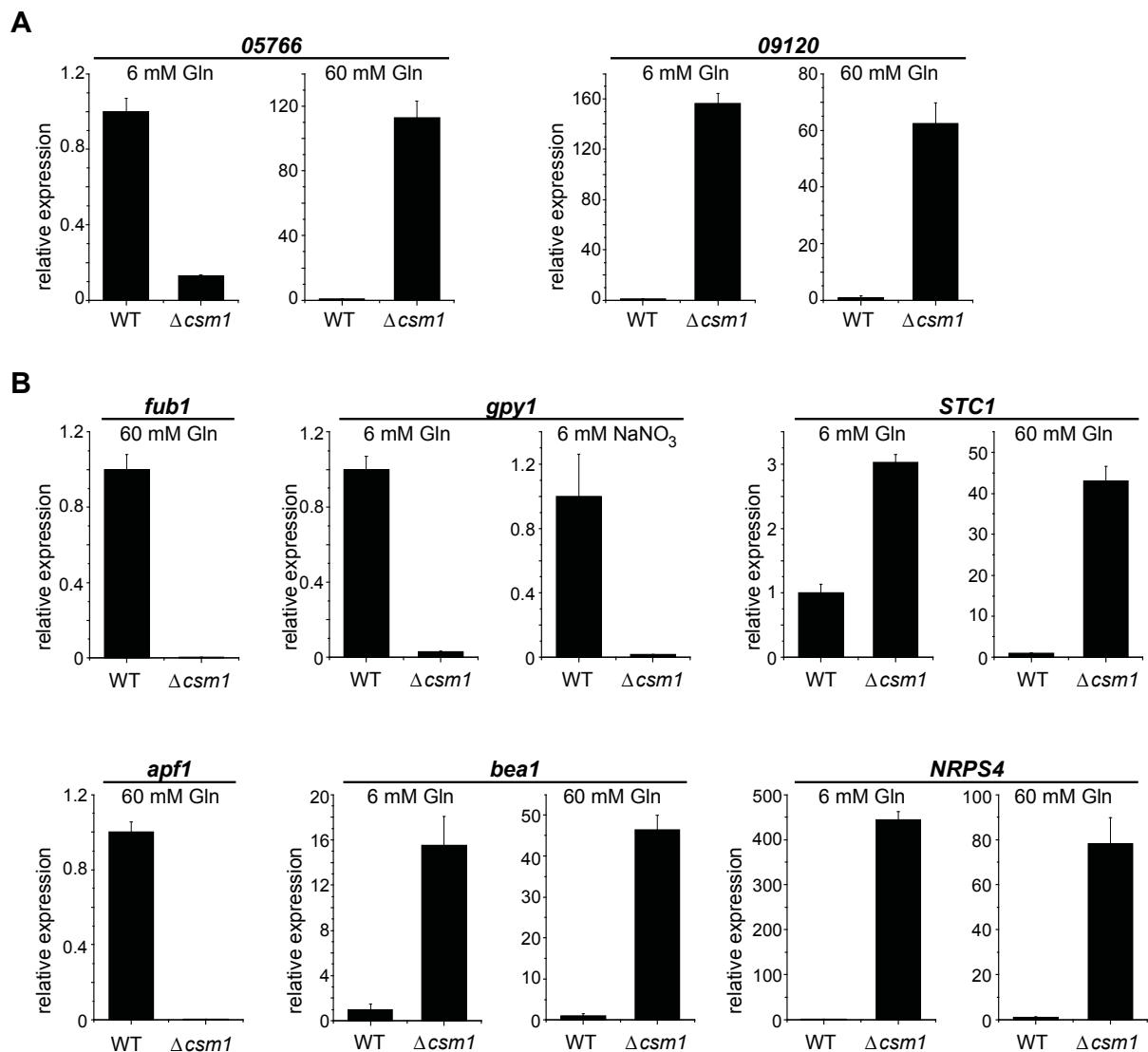


Figure S4: Quantitative real-time PCR (qRT-PCR) analysis of the relative expression of some potential Csm1 target genes using the $\Delta\Delta C_t$ method. The WT and the $\Delta csm1$ mutant were cultivated for 2 d in ICI medium supplemented with either 6 mM or 60 mM glutamine (Gln) or 6 mM NaNO₃. Total RNA from the harvested mycelium was used for cDNA synthesis. Error bars (\pm SD) originate from a technical replicate and expression of the WT was arbitrarily set to 1. **(A)** Expression analysis of the randomly chosen Csm1-dependent transporter genes FFUJ_05766 and FFUJ_09120 encoding an ABC transporter and a putative 4-hydroxybenzoate transporter, respectively (see Table S2). **(B)** Expression analysis of some secondary metabolite key enzyme-encoding genes: *fub1* – encoding the polyketide synthase (PKS) of fusaric acid, *gpy1* – encoding the PKS of gibepyrone, *STC1* – encoding the sesquiterpene cyclase of the putative STC1 cluster, *apf1* – encoding the non-ribosomal peptide synthetase (NRPS) of apicidin F, *bea1* – encoding the NRPS of beauvericin, *NRPS4* – encoding the NRPS of the putative NRPS4 cluster.

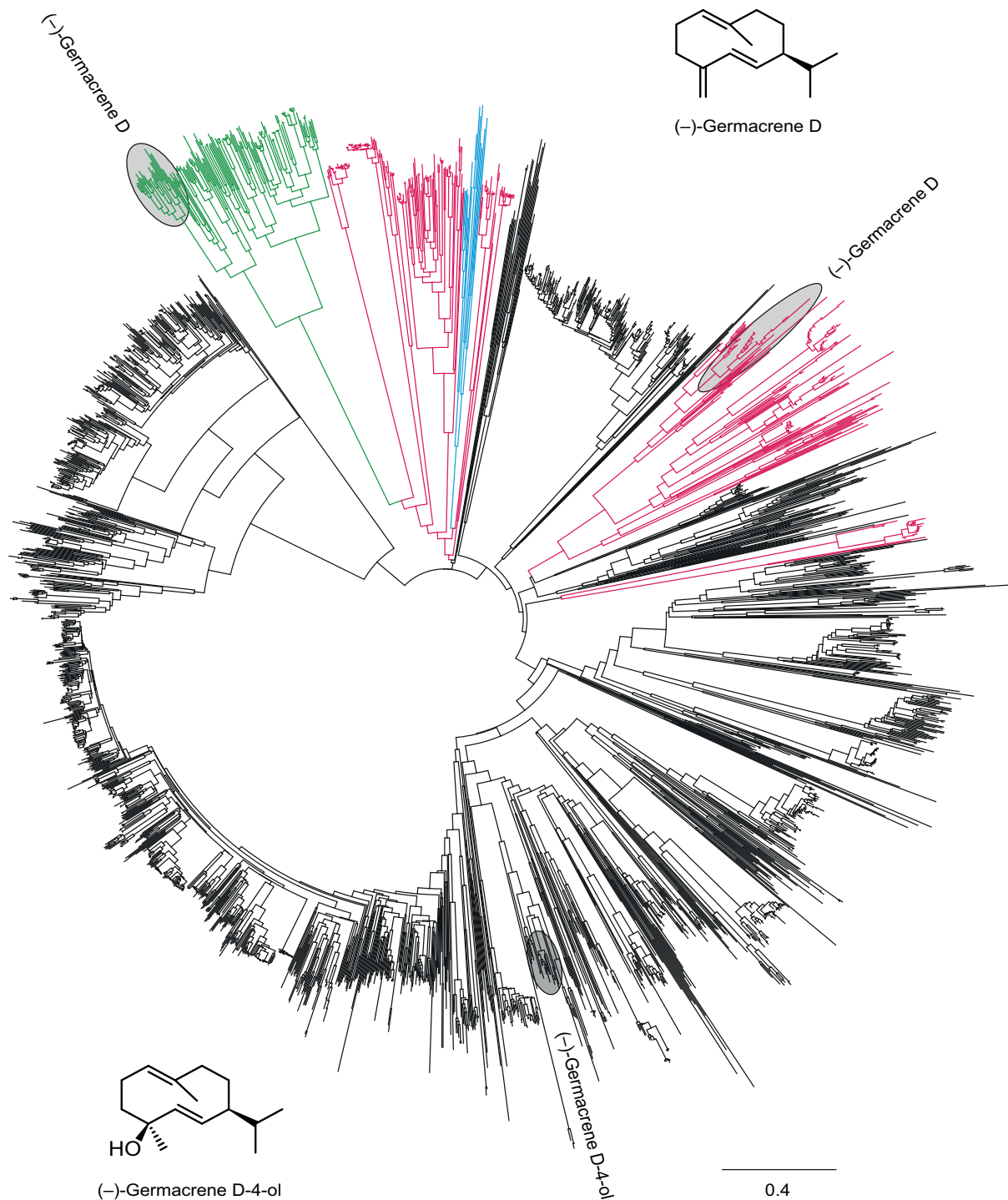


Figure S5: Phylogenetic tree of 2500 terpene cyclase orthologs. The green branches represent plant enzymes, the red branches are fungal enzymes, bacterial enzymes are in black, and the blue branches represent the recently discovered terpene cyclases from social amoebae. The known (-)-germacrene D synthases from plants and fungi and the (-)-germacrene D-4-ol synthases from bacteria are highlighted.